MODELLING DAILY RUNOFF FROM SNOW AND GLACIER MELT USING REMOTE SENSING DATA

J. Schaper and K. Seidel

Computer Vision Group, Communication Technology Laboratory
ETH Zurich, Switzerland
Tel: +41 1 632 42 62, Fax: +41 1 632 12 51, jschaper@vision.ee.ethz.ch

ABSTRACT

In this paper we present runoff simulations for snow and icemelt for the basins of Rhine-Felsberg, Rhône-Sion and Ticino-Bellinzona. We use high resolution multispectral remote sensing data to map snow and ice cover of selected years. Further, we use GIS based extrapolation techniques to evaluate cloud and forest covered areas with respect to snow cover.

We use the deterministic hydrologic model SRM+G to simulate the daily runoff of selected years. Conditions for a norm year in terms of normalized daily values for snow cover depletion, temperature and precipitation for the time period 1961 to 1990 have been established. Based on norm year conditions we did climate change simulations for the scenarios 2030 and 2100, which are characterized by increasing temperatures during winter and summer and increased precipitation during winter. The results show different characteristic behaviour for the three basins. The highly glaciated basin Rhône-Sion shows an influence of enforced summer icemelt, the low glaciated Rhine-Felsberg and Ticino-Bellinzona an earlier snowmelt.

INTRODUCTION

Multispectral optical remote sensing data are particularly qualified for monitoring the extension of the alpine snow and ice cover (1,2,3). The optical satellite sensors are not capable of penetrating clouds, so images with more than 20% cloudiness can not be used for interpretation. However, these problems with partly cloud covered images can widely be mastered since Ehrler showed a method to extrapolate cloud covered areas (4).

Combining the remote sensing derived snow and ice cover maps with a hydrologic runoff model the daily runoff can be calculated (4,5). Snow and icemelt are important contributors to the total yearly runoff volume in high alpine basins. The seasonal snow melts progressively during spring and summer. The snow cover in lower regions of the Alps disappears in March – April, in higher regions in May – August. Sometimes summer new snow delays the ongoing snowmelt. The glacier icemelt results after the glacier areas become snowfree, starting in summer and ending with the autumn snowfall events in September – October. Alpine glaciers are very sensitive to temperature changes because their temperatures lie close to melting point and the refreezing point of water (6). From this point of view it is important to investigate individually the runoff resulting from snow and ice in a warmer climate. Contributing to the research related to snowmelt runoff modelling under the influence of climate change (7,8), we include the glaciermelt in climate change simulations.

The study is carried out for the three Swiss test basins Rhine-Felsberg (3241 km^2, 575 – 3614 m a.s.l.), Rhone-Sion (3371 km^2, 488 – 4634 m a.s.l.) and Ticino-Bellinzona (1515 km^2, 192 – 3402 m a.s.l.) located as shown in Figure 1. The basins are characterized with different topographic, physiographic and climatic conditions. Rhône-Sion is 17% glaciated, Rhine-Felsberg contains just 1.9% and Ticino-Bellinzona has almost no glacier areas (0.5%).

Figure 1: Location of the three alpine basins Rhine-Felsberg, Rhône-Sion and Ticino-Bellinzona in Switzerland.

METHODS

Snow and Ice Cover Mapping Using Remote Sensing

For each alpine basin as mentioned above the snow and ice covered areas have been monitored during the melting season from March – October for various years. Primarily cloud free data sets with 4 – 12 images per season have been chosen from various high resolution satellite sensors like Landsat-MSS, Landsat -TM and SPOT-XS. The imagery was geometrically and radiometrically corrected. Due to the enormous topographic range of the test basins, geometric orthorectification was done with a digital elevation model (DEM 25m resolution). The maximum error amounts to 2 pixels with Landsat and to 4 pixels with SPOT data (in the case of a 19º side-looking sensor). Figure 2 shows an example of an orthorectified Landsat-TM image of the basin Ticino-Bellinzona. The radiometric correction eliminates atmospheric and topographic induced radiation errors and is based on additional scene information and the DEM. We performed this correction with programs of Sandmeier (9). Further, we masked out the cloud and forest covered areas. The forested areas are problematic for snow cover interpretation, since very often the snow is underestimated. We used supervised (maximum likelihood) and unsupervised (K-means clustering) multispectral classification methods to label the pixel, and merged the results to “snow”, “ice”, and “snowfree non-ice”. A first visual inspection pointed to wrong declarations of ice and rocks and, especially in Ticino-Bellinzona, with snow pixel within sparse forest. In a second approach the results have been compared with snow-measurements of SLF (10). Figure 3 shows a result of the classification process in the Ticino-Bellinzona basin.

After classification of the images we extrapolated the cloud and forest covered parts in a geographic information system (GIS) taking advantage of a method developed by Ehrler (4). All images are segmented into *snow cover units* (SCU), being defined as regions of equal snow coverage. Subsequently the forested and cloud covered units are assigned to carry the same snow coverage as

the corresponding forest-free and cloud-free units. The final result is a set of complete classified images for each basin.

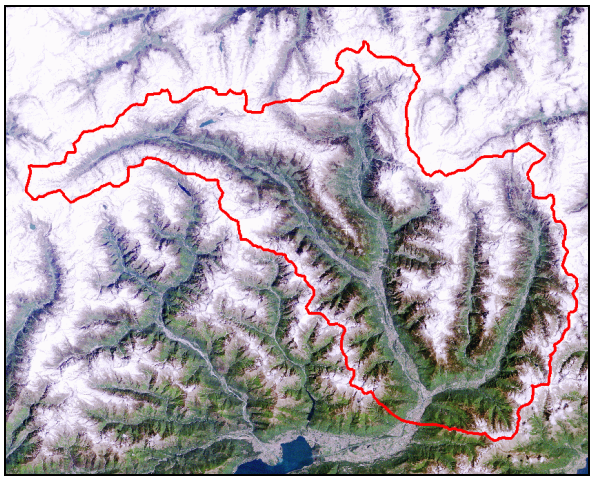

Figure 2: Detail of a Landsat-TM image, channels 3-2-1, from 25-May-1994 showing basin Ticino-Bellinzona (red line). ÓEURIMAGE 1994.

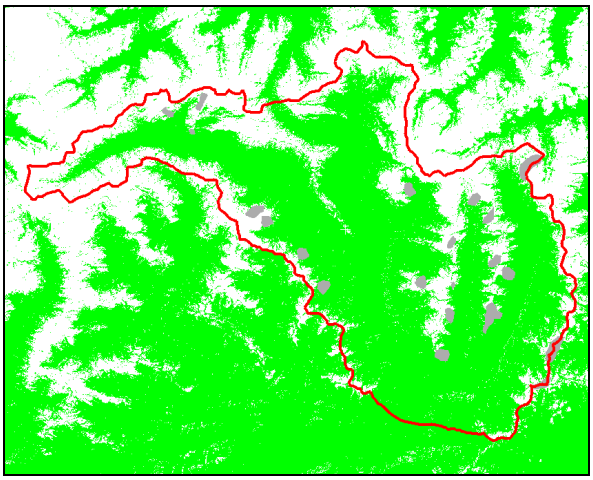

Figure 3: Result from multispectral classification. Snow-free areas are in green, snow covered are white and previously masked clouds appear grey

RUNOFF MODEL FOR SNOW AND GLACIERMELT

The results from remote sensing and GIS were then linked to a hydrologic runoff model. We used the SRM+G model to simulate daily runoff. This model is a further development of the *snowmelt runoff model* (SRM) (5) and can calculate the glaciermelt as well. SRM+G is a deterministic model with spatial distribution in elevation zones and subbasins. The model works with the remote sensing derived snow and ice cover, daily temperature and precipitation measurements and a set of 11 physically derived parameters. The melt computation is based on the degree-day approach, and uses the size and distribution of glaciers within the basin as basic input. To illustrate the procedure, the modified model formula from Martinec (5) can be arranged as follows (11):

$$Q_{n+1} = Q_n k_{n+1} + (1 - k_{n+1}) \cdot \sum_{i=1}^{N} (Q_{\text{rain},n,i} + Q_{\text{newsnow},n,i} + Q_{\text{snowmelt},n,i} + Q_{\text{icemelt},n,i})$$

$$Q_{\text{rain},n,i} = A_{\text{total},i} \cdot c_r \cdot P_r \left[\tfrac{86400}{10000}\right]$$

$$Q_{\text{newsnow},n,i} = A_{\text{total},i} \cdot c_r \cdot a_{n,i} \cdot T_i \cdot (1 - S_{\text{total},i}) \left[\tfrac{86400}{10000}\right]$$

$$Q_{\text{snowmelt},n,i} = (A_{\text{nogl},i} \cdot c_s \cdot a_{n,i} \cdot T_i \cdot S_{\text{nogl},i}) + (A_{\text{gl},i} \cdot c_s \cdot a_{n,i} \cdot T_i \cdot S_{\text{gl},i}) \left[\tfrac{86400}{10000}\right]$$

$$Q_{\text{icemelt},n,i} = A_{\text{gl},i} \cdot c_{gl} \cdot b_{n,i} \cdot T_i \cdot (1 - S_{\text{gl},i}) \left[\tfrac{86400}{10000}\right]$$

$$k_{n+1} = x \cdot (Q_n)^{-y}$$

where Q is the average daily discharge [$m^3 s^{-1}$] with index referring to *rain, newsnow, snowmelt* and *icemelt*. Newsnow indicates snow falling in the summer on a snowfree area whereas snowmelt is the melt of the seasonal snow cover fallen before 1-April. n is an index indicating the sequence of days, c the runoff coefficient expressing the losses through evaporation, interception and sublimation as a ratio (runoff/precipitation) with index referring to *r*ain, *s*now and *gl*acier. a_s is the degree-day factor for snow [cm $^oC^{-1}$ d^{-1}], a_g the degree-day factor for ice [cm $^oC^{-1}$ d^{-1}]. While a_s varies during the melt season accordingly to changing snow density, a_g stays constant over the season. A is the area of a zone [km^2] with index referring to *gl*acier, *nogl*acier and *total* area. The altitude range of the zones is approx. 500 m. T is the air temperature at the mean hypsometric elevation of a zone [^{o}C] and is extrapolated from a network of climate stations with an average temperature gradient of -0.65 ^{o}C per 100 m. P_r is the precipitation as rain according to the critical temperature at the mean

hypsometric elevation of a zone or new snow falling in the summer on snowfree area [cm d^{-1}]. According to the complex precipitation situation of the central alpine valleys it was a challenge to adapt the precipitation gradient to the various climate conditions of the three basins. The precipitation gradient changes from 0 upto 4.5% per 100 m. S is a ratio of the snow covered area to the total area. The recession coefficient k indicates the decline of discharge in a period without snowmelt or rainfall and depends on the storing capacity of the basin. As can be seen from the Eq., k is a function from the constants x and y, which are determined for a given basin from previous years. There are further parameters not listed here, which are described elsewhere (11,12). We tested the model in several basins and found high accuracy even in basins with 67% glacier areas (11).

DERIVATION OF THE NORM YEAR

For each basin runoff simulations were made for selected years within the period 1983 – 1994. In order to compare the basins with each other and to have a basis for calculating climate scenarios, it is important to derive average conditions related to climatic measures and snow cover depletion of the period 1961 – 1990. We performed a normalization of temperature, precipitation and derivation of average snow cover depletion curves and got the values of the so called *norm* year for each basin. The normalization of the meteorological parameters is based on the following formulas:

$$T_{i\text{norm}} = T_i + (\bar{T}_{61\text{-}90} - \bar{T}) \qquad P_{i\text{norm}} = P_i \cdot \frac{\sum P_{61\text{-}90}}{\sum P}$$

where T_i is the daily measured temperature, ($T_{61\text{-}90} - T$) the difference of long time monthly average of the period 1961 –1990 and T the actual monthly mean, P_i the daily measured precipitation, $P_{61\text{-}90}$ the monthly sum of the period 1961 –1990 and P the monthly sum of the actual month. We derived the snow cover of the norm year by reshaping curves of the snow cover depletion from the initial year to the normalized climate conditions.

With the normalized temperature, precipitation and snow cover depletion we calculated the runoff of the norm years. Assigning the runoff to runoff regime nomenclatures of Aschwanden (13), the regime of Rhine-Felsberg is nivo-glacial, of Rhone-Sion b-glacial, and of Ticino-Bellinzona is nival-méridional.

CLIMATE CHANGE SCENARIOS

		Temperature		Precipitation	
		Winter	Summer	Winter	Summer
Rhine-Felsberg	2030	+1.1	+1.2	+5	-
	2100	+3.1	+3.4	+10	-
Rhône-Sion	2030	+0.9	+1.1	+5	-
	2100	+2.9	+3.3	+10	-
Ticino-Bellinzona	2030	+0.9	+1.3	+5	-
	2100	+2.9	+3.5	+10	-

Table 1: Regional climate scenarios based on downscaling of IPCC scenarios (14,15). The shown values refer to the average climate of the period 1961 – 1990. There will be no precipitation changes during summer.

As a further step, we investigated climate change simulations with various scenarios. The two se-

lected scenarios (Table 1) are taken from the Intergovernmental Panel on Climate Change (IPCC) (14) adapted to regional aspects by downscaling (15).

The new snow cover for the climate scenarios has been determined using *modified snow cover depletion curves* (MDC) for each zone reshaping curves from the initial year to the average climatic conditions (Figure 4). MDC characterise the snow cover depletion during the melt season. The MDC contain at the y-axis the extension of the snow cover as derived on certain dates from satellite remote sensing and interpolated by the model [%] and at the x-axis the calculated melt depths as derived from meteorological data [cm]. Changes of the MDC are a measure of a changing snow situation. The initial MDC includes the new snow seen by the satellite, we call this *MDC incl*. Using the SRM+G, we can derive the MDC without new snow, called *MDC excl*. This *MDC excl* can be adapted to a new climate situation. For this purpose the winter snow accumulation of the initial winter and new climate winter are compared. Case 1 shows a situation with less snow accumulation than the initial year, the curve is shifted to the left by the amount of the difference and called *MDC excl wa*. The index *wa* means winter adjusted. Case 2 shows a situation with more winter snow accumulation than the initial year, the curve is scaled with a factor

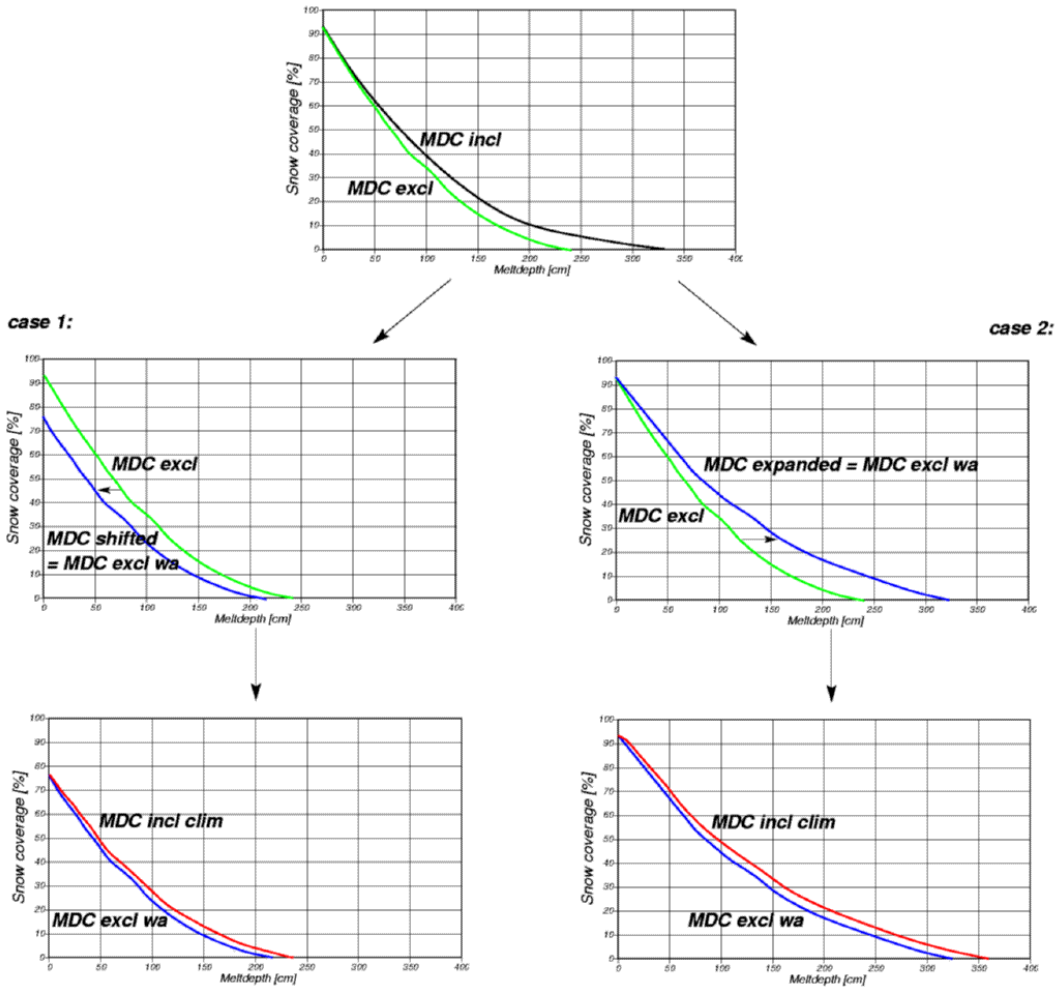

Figure 4: Derivation of the snow coverage for climate change scenarios with modified snow cover depletion curves (MDC). Case 1 shows less snow and case 2 more snow than the initial year. The index incl *means with new snow (seen by the satellite),* excl *means without new snow (substracted by model). Final product is the* MDC incl clim *(red line).*

derived from the difference and called again *MDC excl wa*. As a final step we add with the SRM+G the new snow for the changed climate to the *MDC excl wa* and get the *MDC incl clim*. The whole procedure enables us to react to various snow conditions with data from only one year of satellite derived snow cover situation.

The glacier vector data used in this study are taken from Maisch (16). The data were derived from aerial photographs and field measurements and show an average state of the year 1973 which is a good representation for the norm year. Starting again from this norm year, we calculated the glacier areas for the two scenarios 2030 and 2100 by shifting the 2:1 equilibrium line (EL) according to the summer temperature change given in Table 1. The 2:1 EL assumes a distribution of 2 parts accumulation and 1 part ablation area on the glacier. Therefore the EL will be shifted +150 m per ºC temperature rise. Corresponding to the EL shift we diminished the total glacier area.

Calculating the glacier scenarios for Rhône-Sion with the given summer temperature change, we derived a situation where the glaciers almost dissappeared. The initial glacier area was 619 km^2. The calculated glacier areas for the climate change scenario 2030 was 560 km^2 with an EL rise of 165 m and for the 2100 scenario was 180 km^2 with an EL rise of 495 m. In the case of the more extreme scenario 2100 two thirds of the total glacier area have disappeared.

RESULTS AND DISCUSSION

By modelling the daily runoff for the three basins we observed different trends. As can be seen from Table 2, the yearly runoff volume in the high glaciated Rhône-Sion increases with the scenarios 2030 and 2100 whereas in basins without big glaciers the runoff volume decreases. We attribute this to the influence of the glaciermelt, because more glacier ice is melted than stored in a warming climate. The glacier areas in the other two basins are so small that they do not affect the total runoff amount at the gauge station. It can be stated, that the runoff amount of scenario 2100 is higher than 2030 in Rhône-Sion and Ticino-Bellinzona, but less in Rhine-Felsberg. This is a consequence of the runoff composition resp. of the runoff regimes (see previous chapter). Both glacial regimes of Rhine-Felsberg and Rhône-Sion show only a low influence of winter precipitation. However, the regime of Ticino-Bellinzona is nival-méridional, which means that the influence of October precipitation is in second position of the monthly ranking. The reason for the high runoff volume in 2100 in Rhône-Sion is the increasing glaciermelt and in Ticino-Bellinzona the effect of the increase of winter precipitation. Rhine-Felsberg has neither big glacier areas nor high winter precipitation.

	Rhine-Felsberg	Rhône-Sion	Ticino-Bellinzona
Q norm year	$3882 \cdot 10^6$ m^3	$3288 \cdot 10^6$ m^3	$2314 \cdot 10^6$ m^3
Q 2030	$3596 \cdot 10^6$ m^3 (– 7.4%)	$3631 \cdot 10^6$ m^3 (+10.4%)	$2127 \cdot 10^6$ m^3 (– 8.1%)
Q 2100	$3515 \cdot 10^6$ m^3 (– 9.4%)	$3704 \cdot 10^6$ m^3 (+12.7%)	$2168 \cdot 10^6$ m^3 (– 6.3%)

Table 2: Results of runoff modelling for norm years and scenarios. The high glaciated Rhône-Sion shows different behaviour as the low glaciated Rhine-Felsberg and Ticino-Bellinzona.

Based on Figures 5+6, the hydrographs for the scenario 2100 differ massively from the norm hydrographs. The hydrograph of Rhine-Felsberg is not printed here, but looks similar to Ticino-Bellinzona. The Rhône-Sion hydrograph shows more runoff in winter and spring, but less in summer and autumn. This indicates a shift from winter snowfall to winter rain and means that part of the winter precipitation is no longer stored in the seasonal snow cover, but becomes promptly effective to the runoff. This amount of water is not available during the summer. Furthermore we can observe a seasonal shift of snowmelt from summer to spring time, both due to the temperature in-

crease. The runoff contribution from the glaciers is increasing. This process will continue as long as the main part of the glaciers is melting.

The Ticino-Bellinzona hydrograph for scenario 2100 shows more runoff during wintertime, two significant peaks in April and May and much less runoff in June and July. As with the other basins, the winter precipitation appears in the scenarios more often in the form of rain than of snow fall, although the evaporation is higher in the warming climate.

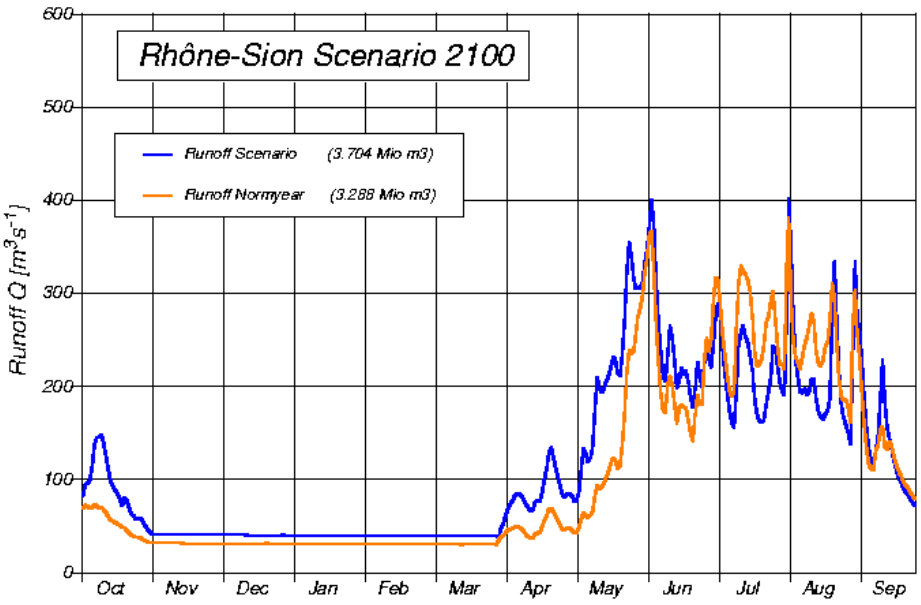

Figure 5: Runoff computation for basin Rhône-Sion. The hydrograph for scenario 2100 (blue line) shows a higher volume than for the norm year (orange line).

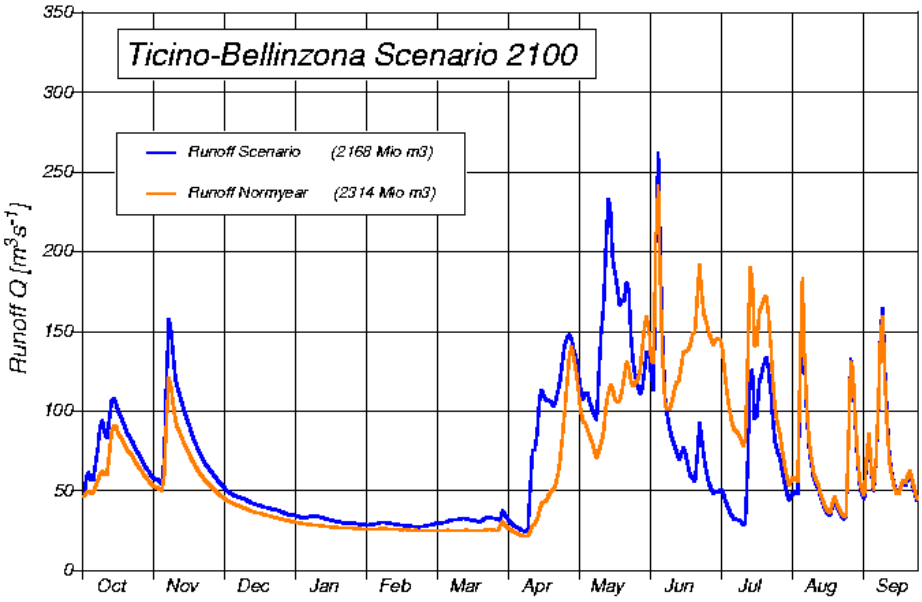

Figure 6: Runoff computation for basin Ticino-Bellinzona. The hydrograph for scenario 2100 (blue line) shows a lower volume than for the norm year (orange line).

CONCLUSIONS

- The study shows a method to calculate runoff from snow- and icemelt using meteorological data and remote sensing derived snow and ice cover maps.
- In order to compare different regions with each other we derived norm year conditions for snow cover depletion, temperature and precipitation.
- Climate change scenarios for warming climate show different impacts on the three basins, depending on the basin characteristics and the degree of glaciation.

ACKNOWLEDGMENTS

The authors would like to thank M. Maisch from the Dept. of Geography of the University of Zurich for providing the glacier boundary data. This work has been carried out with the support of the Swiss National Science Foundation (NFP Grant 21-53539).

REFERENCES

1. Hall, D., Riggs, G. and Salomonson, V. 1995. Development of methods for mapping global snow cover using moderate resolution imaging spectroradiometer data. *Remote Sensing of Environment*. (54):127 – 140.
2. Rango, A. 1996. Spaceborne remote sensing for snow hydrology applications. *Hydrological Sciences*. 41(4):477 – 494.
3. Haefner, H., Seidel, K. and Ehrler, C. 1997. Applications of snow cover mapping in high mountain regions. *Physics and Chemistry of the Earth*, 25:275 – 278.
4. Ehrler, C., Seidel, K. and Martinec, J. 1997. Advanced analysis of snow cover based on satellite remote sensing for the assessment of water resources. Proceedings of the IAHS Symposium: Remote Sensing and Geographic Information Systems for Design and Operation of Water Resources Systems, Rabat, Morocco, IAHS Publ. 242, 93 – 101.
5. Martinec, J. 1975. Snowmelt-runoff model for streamflow forecasts. *Nordic Hydrology*. 6:145 – 154.
6. Beniston, M., Haeberli, W., and Schmid, E. 1998 Wie empfindlich reagieren Gebirgsregionen auf klimatische Veränderungen. In: Lozán, J., and Grassl, H. , and Hupfer, P. (Ed.) Warnsignal Klima, Wissenschaftliche Fakten. Hamburg.
7. Gleick, P. 1986. Methods for evaluating the regional hydrologic impacts of global climatic changes. *Journal of Hydrology*. 88:97 – 116.
8. Ehrler, C., Seidel, K. 1995. Mutual Effects of the Climate Change and the Alpine Snow Cover and their Influence on the Runoff Regime Evaluated with the Aid of Satellite Remote Sensing. IGARSS'95; Quantitative Remote Sensing for Science and Applications:_1973-1975. Florence, Italy.
9. Sandmeier, S. 1995. A physically-based radiometric correction model. Correction of atmospheric and illumination effects in optical satellite data of rugged terrain. *Remote Sensing Series 26*, University of Zürich, Dept. of Geography.
10. SLF: Schnee und Lawinen in den Schweizer Alpen. Winterbericht des Eidgenössischen Instituts für Schnee- und Lawinenforschung, Davos (annual).
11. Schaper, J., Martinec, J., and Seidel, K. 1999. Distributed Mapping of Snow and Glaciers for Improved Runoff Modelling. *Hydrological Processes*, 13(12-13):2023-2031.
12. Schaper, J., Seidel, K. and Martinec, J. 2000. Precision snow cover and glacier mapping for runoff modelling in a high alpine basin. Remote Sensing and Hydrology 2000. Proc. of the Santa Fe symp., Apr. 2000, IAHS Publ. No. 268. in press.

13. Aschwanden, H. , and Weingartner, R. 1985. Die Abflussregime der Schweiz. Publikation Gewässerkunde des Geogr. Inst. der Univ. Bern. (65).
14. WMO-UNEP 1990. Intergovernmental Panel on Climate Change (IPCC). Potential Impacts of Climate Change. Report prepared for IPCC by Working Group II. WMO, Geneva.
15. ProClim-Forum 1995. Climate change: The IPCC second assessment report, impacts and response strategies. Bern. 68 pp.
16. Maisch, M. *et al.* 1999. Die Gletscher der Schweizer Alpen – Gletscherstand 1850 – Aktuelle Vergletscherung – Gletscherschwund-Szenarien. NFP 31 Schlussbericht. vdf Hochschulverlag an der ETH Zürich. 373 pp.